



This is a repository copy of *Finite-element analysis on cantilever beams coated with magnetostrictive material*.

White Rose Research Online URL for this paper:  
<http://eprints.whiterose.ac.uk/3614/>

---

**Article:**

Dean, J., Gibbs, M.R.J. and Schrefl, T. (2006) Finite-element analysis on cantilever beams coated with magnetostrictive material. *IEEE Transactions on Magnetics*, 42 (2 (par)). pp. 283-288. ISSN 0018-9464

<https://doi.org/10.1109/TMAG.2005.861322>

---

**Reuse**

Unless indicated otherwise, fulltext items are protected by copyright with all rights reserved. The copyright exception in section 29 of the Copyright, Designs and Patents Act 1988 allows the making of a single copy solely for the purpose of non-commercial research or private study within the limits of fair dealing. The publisher or other rights-holder may allow further reproduction and re-use of this version - refer to the White Rose Research Online record for this item. Where records identify the publisher as the copyright holder, users can verify any specific terms of use on the publisher's website.

**Takedown**

If you consider content in White Rose Research Online to be in breach of UK law, please notify us by emailing [eprints@whiterose.ac.uk](mailto:eprints@whiterose.ac.uk) including the URL of the record and the reason for the withdrawal request.



[eprints@whiterose.ac.uk](mailto:eprints@whiterose.ac.uk)  
<https://eprints.whiterose.ac.uk/>

# Finite-Element Analysis on Cantilever Beams Coated With Magnetostrictive Material

J. Dean, M. R. J. Gibbs, and T. Schrefl

Sheffield Centre for Advanced Magnetic Materials and Devices, Department of Engineering Materials, University of Sheffield, Sheffield S1 3JD, U.K.

The main focus of this paper is to highlight some of the key criteria in successful utilization of magnetostrictive materials within a cantilever based microelectromechanical system (MEMS). The behavior of coated cantilever beams is complex and many authors have offered solutions using analytical techniques. In this study, the FEMLAB finite-element multiphysics package was used to incorporate the full magnetostrictive strain tensor and couple it with partial differential equations from structural mechanics to solve simple cantilever systems. A wide range of geometries and material properties were solved to study the effects on cantilever deflection and the system resonance frequencies. The latter were found by the use of an eigen-frequency solver. The models have been tailored for comparison with other such data within the field and results also go beyond previous work.

*Index Terms*—Finite-element modeling, magnetostriction, magnetostrictive actuator, microelectromechanical system (MEMS).

## I. INTRODUCTION

THE current development and technology for micrometer-sized devices have been facilitated by multidisciplinary areas of research, producing devices based on mechanical, optical, electrical, magnetic, and fluidic systems. There have been significant advances in recent years in constructing micrometer scaled devices based on electrical and mechanical systems and there is growing commercial interest. In 1999, devices on the micrometer scale were primarily used for sensing and actuator functions, with the U.S. market value in the \$100 million range [1]. The advancement of this technology is being used in many other processes, with the worldwide market thought to exceed \$8 billion in the next two years and predicted to increase at a rate of 20% per year, as automotive and telecommunications drive the applications forward. Within the field of microelectromechanical systems (MEMS), the incorporation of magnetic materials is presenting a new category of MagMEMS, adding new capabilities and opening up new markets within biomedical, astronomy, and information technology [2], [3].

A magnetostrictive material is one that develops mechanical deformations when subjected to an external magnetic field, and magnetostriction is an effect present in ferromagnetic materials that undergo part or all of the magnetization process by moment rotation as opposed to domain wall movement [4], [5]. In response to a magnetic field, the moments will begin to rotate toward the field. In general, this changes the total free energy of the system. The material will minimize this change with adjustments to the bond length between constituent atoms and an internal strain may be generated within the material. This internal strain increases until saturation is achieved. In devices such as switches, valves, or sensors, magnetostriction has merits over piezoelectric elements due to a higher power density, remote actuation, lower performance degradation, simpler fabrication processes, higher response time, and the ability to remotely operate without electrical contacts [3], [6], [7]. Bimorphs are one

of the basic structures in MEMS and are used as devices, but also for analysis methods such as the calibration of the magnetostriction constants within magnetic materials [8], [9]. These devices are fabricated using lithographic techniques with sacrificial layers to form an armature that is pinned rigidly at one end. Successful utilization depends on the ability to fully understand the properties and intrinsic interactions these materials and structures possess, and how they can be incorporated efficiently into practical devices.

## II. BACKGROUND

Many authors have worked on a complete mathematical formalism for magnetostriction by finding the energy stored within the material. Work performed by Chikazumi [10], Kittel [11], and du Trémolet de Lacheisserie [5], [12]–[14], among others used the minimization of the internal energy to find the internal strain generated by an external magnetic field. Inconsistencies found within these derivations by Guerrero and Wetherhold [15], [16] were overcome by minimizing the Gibbs free energy density,  $g$ , as defined in (1). This form incorporates the total internal energy  $U_{\text{tot}}$  with the stress and strain tensors,  $\tau_{ij}$  and  $\varepsilon_{ij}$ , respectively

$$g = U_{\text{tot}} - \tau_{ij}\varepsilon_{ij} \quad (1)$$

$$\varepsilon_{ij}^e = \begin{pmatrix} \frac{3}{2}\lambda_{100}(\alpha_x^2 - \frac{1}{3}) & 3\lambda_{111}(\alpha_x\alpha_y) & 3\lambda_{111}(\alpha_x\alpha_z) \\ 3\lambda_{111}(\alpha_y\alpha_x) & \frac{3}{2}\lambda_{100}(\alpha_y^2 - \frac{1}{3}) & 3\lambda_{111}(\alpha_y\alpha_z) \\ 3\lambda_{111}(\alpha_z\alpha_x) & 3\lambda_{111}(\alpha_z\alpha_y) & \frac{3}{2}\lambda_{100}(\alpha_z^2 - \frac{1}{3}) \end{pmatrix}. \quad (2)$$

It followed that by the minimizing of (1), the strain tensor was realized, as shown in (2). The matrix can be used to identify the mechanical strains  $\varepsilon_{ij}^e$  generated from the application of an external magnetic field in a direction given by the directional cosines  $\alpha_{ij}$  relative to the crystallographic axes. The magnitude of the strain is proportional to the magnetostriction constant of the material  $\lambda$ , and is dependent on the structure and crystal orientation. This tensor is of the exact same mathematical form

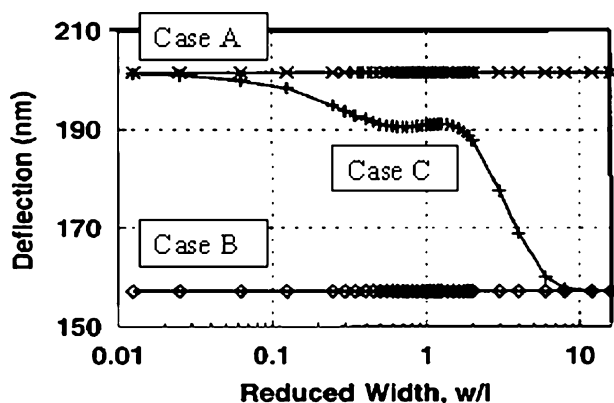


Fig. 1. Two analytical solutions, Case A [12]–[14] and Case B [17], [18] compared against FEM modeling (Case C) of the deflection of the center of a coated cantilever beam. Taken from Watts *et al.* [20].

as previous authors' work [5], [10]–[14]; however, these were classified as macroscopically observed strains  $\varepsilon_{ij}$ . The ability to now class this matrix tensor as mechanical internal strains, allows the ability to use similar solving methods that have been developed for elastic materials, and also allows the simple incorporation and coupling of other internal strains within the same system. These could range for example as strains generated from piezoelectric materials and thermal expansion.

From (2), if the magnetic field is directed along a crystallographic axis, the shear terms drop out leaving a nonzero diagonal with a maximum strain that is directed in line with the magnetic field. This maximum strain will be in the direction of the applied magnetic field with an opposite strain present along the other two axes. This importance of this effect and the way it translates to the magnetic material and its response to magnetic fields is crucial in understanding the deflections of any device.

Previous authors such as du Trémolet de Lacheisserie [5], [12] and Marcus [17], [18] have used the minimization of internal energy and the same general magnetostrictive tensor to develop analytical models for the solutions to the deflection of cantilever beams. The model developed by du Trémolet de Lacheisserie *et al.* [5], [12]–[14], [19] was solved for a system that is free to flex across the width. This system was solved using a pinned single node in the center of one edge implemented with zero degrees of freedom, shown in Fig. 1 as case A. A different boundary condition employed by Marcus [17], [18] modeled a similar type of system but with all nodes within the system unable to bend across the width, shown as case B in Fig. 1. One important feature to note is that these models are both independent of cantilever width.

Finite-element modeling by Watts *et al.* [20] on the same cantilever system found that the center deflection was not as simple as predicted by the analytical solutions, as shown by case C in Fig. 1. The actual center deflection was between these two limiting cases with a high width to length ratio ( $w/l$ ) tending toward case B, and low  $w/l$  tending to case A. The model was solved using the ANSYS package and limited within the application due to the model having to use thermal expansion with appropriate expansion coefficients to approximate the magnetostriction strain.

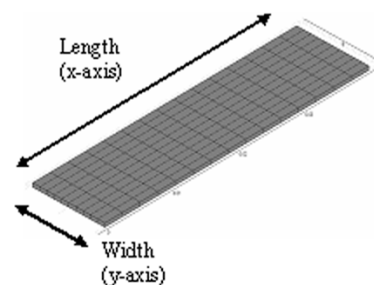


Fig. 2. A simple cantilever meshed with 400 quadrilateral elements causing 20 000 degrees of freedom. The cantilever is pinned across the width on one edge boundary.

The development of the multiphysics finite-element package FEMLAB [21] allows the magnetostrictive strain tensor to be implemented directly using the actual properties of the materials involved within the system. We now discuss this implementation, and the new insights it provides.

### III. FEMLAB MODEL

The use of finite-element modeling packages for modeling systems has dramatically increased with the spread of faster personal computers. The development of cheaper packages such as ANSYS and FEMLAB has increased the potential for modeling devices. FEMLAB 3.0a incorporates its own solver and can be used as a standalone package encompassing a solid modeling engine, the meshing algorithms and a selection of solvers. This package has the ability to create two- and three-dimensional models which can be solved for linear and nonlinear, stationary, and time dependent situations, with the capability to perform eigen-value analysis on them. It also has the capability to combine and couple different partial differential equations (PDEs) from areas of physics such as stress-strain to the incompressible Navier–Stokes equations.

FEMLAB incorporates many ways of solving PDEs. The simplest is a coefficient form and is applicable to linear or near linear models; however, due to the complexities of this model a nonlinear solver is required that uses a general or weak solution forms. Along with the PDE solver, FEMLAB also incorporates an eigenvalue solver to handle linear eigenvalue problems and the ability to analyze the frequency response of structures.

Owing to FEMLAB's limitations for the meshing of large dimensional thickness ratios between two layers in one model, such as the case of a thin film on a much thicker substrate, a simple regimented quadrilateral meshing element is favored over the tetrahedral 3-D mesh generation using the Delaunay algorithm. The quadrilateral element structure is sufficient for a simple square cantilever and allows for significantly faster solving times compared to that of tetrahedral elements due to the reduction in the number of nodes from on average 200 000 to 400 with no significant difference between the solutions. The simple model is shown in Fig. 2 showing the quadrilateral meshing elements.

To set up the model, a MEMS application mode containing the structural mechanics PDEs are used. This has the ability to solve problems using the stress-strain relationship for elastic materials with structures down to the nano-scale. The strain

within the system can be described, at a point, by the dependent variables for the displacement components  $u$ ,  $v$ , and  $w$ . The total strain within the system can also be broken down to three additive components of thermal, elastic, and internal strain. The implementation of the magnetostrictive tensor is used within the internal strain of the PDE. The significance of using the magnetoelastic strain within a FEM model is that it requires no approximations within the PDE for changes in the plate layer and reduced width ratios. If working with thicker plates, however, a higher density of mesh elements should be introduced into the thickness direction to achieve suitable convergence. The effect of thickness on the cantilevers deflection is at present an ongoing study.

To construct the cantilever, a rectangle to the chosen dimensions of width and length is first drawn in two dimensions, meshed using the quadrilateral elements and extruded in to three dimensions. The mesh extrusion is carried out for two separate layers, the first being for the thickness of the substrate, usually in micrometers, the second for the film thickness. Hence once extruded, two separate subdomains are available for solving, one representing the substrate and the other the film. The material properties such as the Young's modulus, Poisson's ratio, and density are then implemented and linked to the appropriate subdomain.

The magnetostriction strain tensor is then incorporated into the strain-stress PDE for the active magnetic layer only. The nodal points on one edge of both the domains are then given the property of zero degrees of freedom, effectively pinning the edge of the structure to form the cantilever beam.

As this system is a complex system of strains, a stationary nonlinear solver was used with a relative tolerance for the convergence set at  $10^{-6}$ . This solver uses an invariant form of the damped Newton method whereby an initial estimate to the solution  $U_0$  is used [22]. The algorithm solves a linear system to form a correction  $\delta U$ . A new estimate to the solution is formed from this correction which can be iterated until convergence is reached. To avoid systems that do not converge, an upper limit of 25 iterations is employed, however, all results obtained within this paper from FEMLAB have converged before this upper limit is reached.

In addition to this stationary solver, an eigenvalue and frequency response solver are also implemented on the model to find the undamped resonances within the cantilever systems and the steady-state response to harmonic loads, respectively.

Once the solver had converged, the results can be post-processed. These can be shown in various formats; however, for simplicity and quickness a boundary visualization is employed, whereby the solved nodes on the boundary of each surface are used to display the expression desired. As the demagnetized state of a sample is undefined, two identical models are set up and solved simultaneously with the directional cosines of the magnetization set along the  $x$  and  $y$  axes, respectively. The post-processed results shown within this report for all the models are presented as the difference between these two orthogonal states. This represents the maximum magnetostrictive strain which can be generated by pure moment rotation through  $90^\circ$ .

For differing finite-element modeling packages and their solved solutions, a number of problems can lead to differences

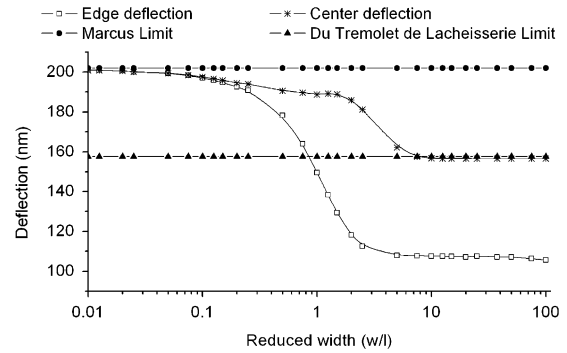


Fig. 3. Deflection of a Permalloy on a glass substrate compared to previous analytical solutions.

between the final converged answer for the same set problem. The main source of this discrepancy is that of numerical errors within the program, such as from the results of the differing calculation procedures including truncation and rounding errors throughout the convergence sequence. Other sources of problems can be the optimization of meshing the structure, the degree of accuracy of the convergence, and the degree of accuracy of constants used with the software leading to, in some models, a discrepancy of up to 10%.

#### IV. CANTILEVER AND DEFLECTION

In Fig. 3, the results from the FEM model developed on FEMLAB are shown and compared to the limiting solutions as shown in Fig. 1. Using 72 nm of Permalloy on a 400  $\mu\text{m}$  glass substrate, as per Watts [20], a nonuniform deflection is produced between the center and edge of the structure. This comparison between the FEM model performed in FEMLAB and the ANSYS model performed by Watts *et al.* in Fig. 1 is well within the standard 10% error.

The two limiting case models described above also agree with the deflection obtained from this new modeling, at extreme geometries for the deflection of the center regions only.

At a large reduced width, there is a significant difference between the center and edge deflections. This represents curling of the end of the cantilever, and is a significant contribution to the overall deflection until a reduced width of 0.1. The stiffness of the geometry of the structure governs this reduction in curling, forming a flatter ended cantilever.

As  $w/l$  approaches zero, the deflection for the edge and center begin to converge toward the same value and the du Trémolet de Lacheisserie limit. For this system, shown in Fig. 4(a), a change of 0.5 nm across the width is observed. At larger  $w/l$  values, there is a noticeable difference for the deflection with only the center values converging to the Marcus limit. The far edges of this shape of cantilever are able to flex by over 60 nm as highlighted in Fig. 4(b).

As  $w/l$  approaches unity the central deflection appears to be pinned due to the shape stiffness with a 40 nm change across the width, as shown in Fig. 4(c). As the silicon substrate is stiffer than the magnetic material, this governs the development of the deflection, forcing just the edges to bend until the strain is great enough in the active material to overcome the stiffness of the

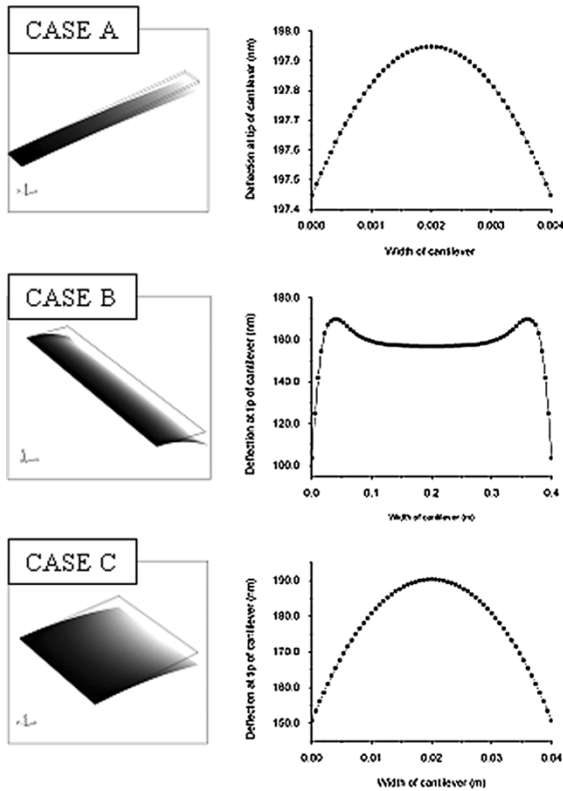


Fig. 4. Change in deflection at three main points of the  $w/l$  ratio using a 4 mm wide cantilever coupled with the material properties from as given by Watts [20]. The graph by each image highlights the deflection of the free end across the width. The  $w/l$  ratios of 10, 0.1, and 1 are for cases A, B, and C, respectively.

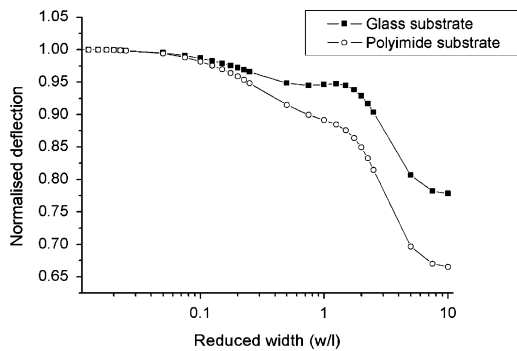


Fig. 5. Normalized comparison in the deflection at the center of a cantilever with two differing substrates.

silicon. Thus, the plateau increases as the active layer becomes less dominant.

The dependence of the deflection characteristics on the substrate is shown in Fig. 5, where comparisons between different substrates are overlaid. The first system utilizes a 400  $\mu\text{m}$  glass substrate while the other uses a Kapton polyimide substrate of the same thickness. Both systems are then effectively coated with 100 nm of Permalloy as the active magnetic material. The reduction in the extent of the plateau is clearly visible due to the reduced stiffness of the substrate. Additionally the ratio of the edge to center deflection for a  $w/l = 10$  for glass and Kapton sees a 0.685 and 0.649 change, respectively. Although a slight increase is experienced due to the stiffer substrate, this still suggests that the curling of the edges is an inherent shape problem of the cantilever system and not due to the materials within the system.

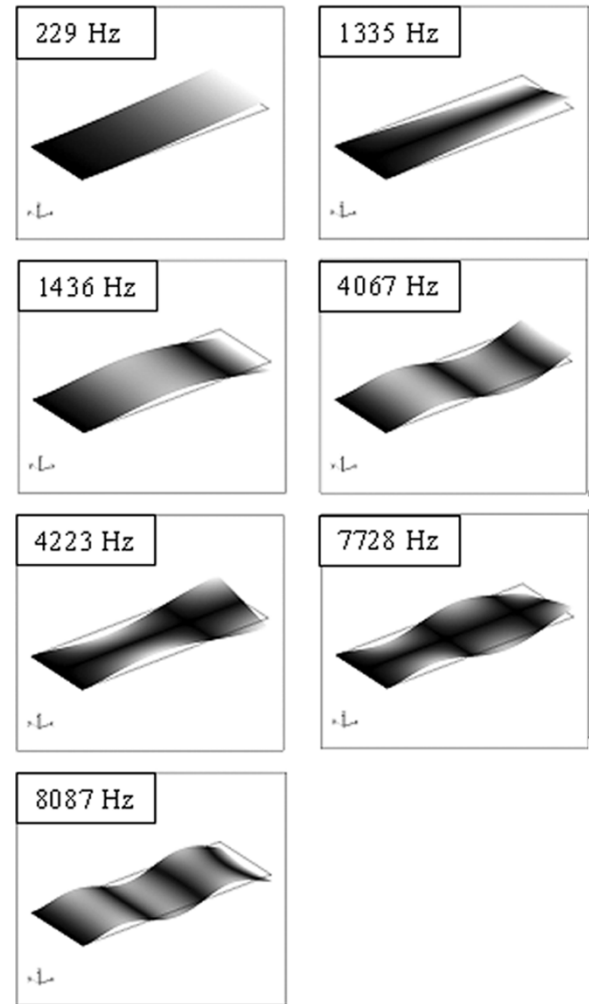


Fig. 6. The first seven eigen-frequencies of the cantilever system using the properties as used by Guerrero and Wetherhold [22]. Note: Dark areas indicate zero deflection and white maximum deflection.

## V. FREQUENCY RESPONSE

The frequency response solver can be implemented on to any model to find the mechanical response of the system. To compare with previously published values, a cantilever of 23 mm  $\times$  8.5 mm was generated following analytical solutions by Guerrero and Wetherhold [23].

The structure has a  $w/l$  ratio of 0.37 corresponding to a system with reduced curling due to shape stiffness. Material properties of the structure were set as a glass substrate of 150  $\mu\text{m}$  coupled with an active layer of 1.1  $\mu\text{m}$  implemented with the properties of the magnetostrictive Tb-Fe alloy Terfenol D [24].

The eigensolver was then used to find the frequencies of the system. The solver was able to calculate not only the pure bending frequencies of the system but also the torsional modes.

Within this system, the first seven resonance modes in order of increased frequency were solved which included four pure bending modes and three torsional ones as shown in Fig. 6. The solved values of the first seven eigen-solutions are within 5% of published analytical data [23] given as 229 Hz, 1332 Hz, 1429 Hz, 4014 Hz, 4208 Hz, 7624 Hz, and 7892 Hz.

Fig. 7, shows the amplitude of the cantilever deflection as a function of frequency. The peaks correspond to the first three

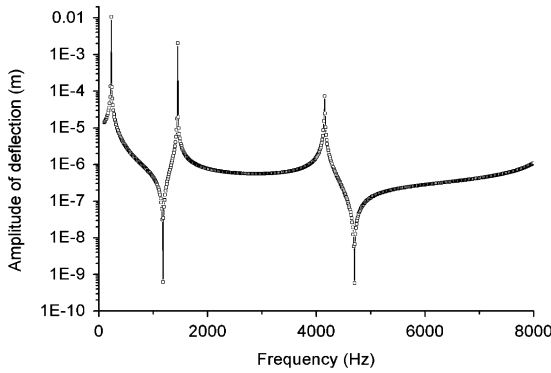


Fig. 7. Frequency response of a cantilever system as a function of frequency where the magnetic field is only directed along the length of the system producing only longitudinal modes of bending.

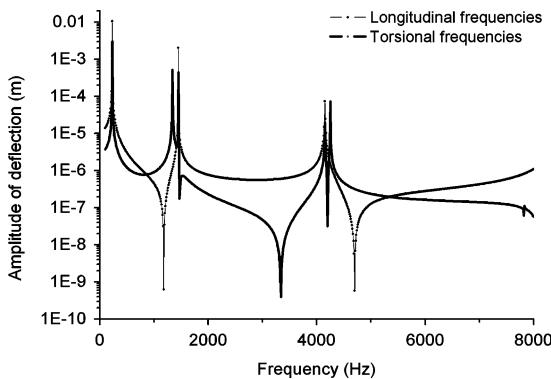


Fig. 8. Comparison of the cantilever frequency with a  $45^\circ$  magnetic field applied.

longitudinal bending modes, as the magnetic field has been applied along the length of the system, setting  $\alpha_x = 1$  in (2). This, due to the magnetostrictive matrix, only introduces longitudinal modes as no torsional strain is induced. These modes are spaced out in frequency, and no coupling between them would be expected.

Introducing a rotating magnetic field causes torsional oscillations. To simplify the model, a magnetic field set at  $45^\circ$  was used,  $\alpha_x^2 + \alpha_y^2 = 1$  in (2), and is shown overlaid on the pure bending modes in Fig. 8.

The resonant frequency of the longitudinal bending modes are unaffected by the incorporation of a torsional force; however, the first twisting and second twisting modes are very close to the second and third bending modes, respectively. One other important point to note is the inclusion of the shear bending terms effects the amplitude of the cantilever's deflection. This change will be as a function of angle, an issue if a rotating magnetic field is used.

To compare how these mechanical resonances are dependent on width the first five bending modes were plotted as a function of reduced width as shown in Fig. 9.

Although only the first five eigen-frequencies are plotted, some important features are still present. The pure bending modes are shown to be independent of the width, with the torsional frequencies highly dependent on any change in width. This would cause problems for cantilever systems that use rotating magnetic fields and analyze the resonance frequency

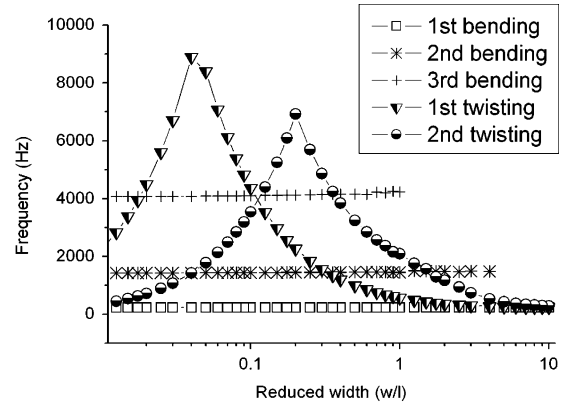


Fig. 9. First five eigen-frequencies of the cantilever system plotted as a function of width.

for a response. At certain  $w/l$  ratios, torsional and bending frequencies are close to each and at some points cross, leading to possible deflection anomalies if driven close to these frequencies causing the bimorph cantilever to become unstable.

## VI. CONCLUSION

The finite-element modeling presented here highlights two major problems with coated cantilever beams that should be addressed in any design stage.

The deflection of the edges to the center at the tip of magnetic coated cantilevers is crucial for any devices used as a switches, valves, or pump. This would also cause problems in the technique of calibration of magnetostrictive constants using actuators. The deflection of the beam used, if care is not taken, could introduce significant errors due to the curling. One way to over this problem would be to limit the curling by introducing shape stiffness; however, care should be taken when working with low  $w/l$  ratios as this would expose other problems to the system, most notable the effect this has on the harmonic series of resonance frequencies.

The torsional mechanical resonance frequencies of cantilevers are highly dependent on width, at low  $w/l$  ratios, a high number of these frequencies are close together. If used with ac fields and the system not tailored correctly, stability issues could arise. However, if designed correctly, these extra torsional modes could be beneficial.

This method of modeling is a robust and simple way of modeling magnetostriction within MEMS. This system can be used not only to calculate the static behavior experienced by differing materials, but also the natural frequencies of the plates and the dynamic behavior. FEMLAB also incorporates the ability to mesh thin structures and much larger structures together and the capability to change any boundary conditions with relative ease. This allows structures such as membranes and bridges to be generate as simply as the cantilever structure. The use of the 2-D geometry extruded to a 3-D shape allows complex structures to be built in layers, with the potential to draw any shape.

One important benefit of FEMLAB is the opportunity to easily couple other partial differential equations to the system with specific boundary conditions to the magnetostrictive model. This would allow the possibility to design a complete

MEMS system with the ability to analyze, for instance, the deflection and frequency dependence as shown here, along with thermal expansion and fluidic and heat flow.

#### ACKNOWLEDGMENT

This work was supported in part by the EPSRC doctoral training account in the Department of Engineering Materials, University of Sheffield.

#### REFERENCES

- [1] J. E. Gulliksen, "MEMS: Where are we," *SemiConduction Mag.*, vol. 1, no. 10, 2000.
- [2] O. Cugat, J. Delamare, and G. Reyne, "Magnetic micro-actuators and systems (MAGMAS)," *IEEE Trans. Magn.*, vol. 39, no. Sep., pp. R3607–R3612, 2003.
- [3] M. R. J. Gibbs, E. W. Hill, and P. J. Wright, "Magnetic materials for MEMS applications," *J. Phys. D, Appl. Phys.*, vol. 37, no. 22, pp. 237–244, 2004.
- [4] R. C. O'Handley, "Modern magnetic materials principles and applications," in *Wiley-Interscience*: New York, 2000, pp. 218–239.
- [5] E. Du Trémolet de Lacheisserie, *Magnetostriction: Theory and Applications of Magnetoelasticity*. Boca Raton, FL: CRC, 1993.
- [6] J. W. Judy, "Microelectromechanical systems (MEMS): Fabrication, design and applications," *Smart Mater. Struct.*, vol. 10, pp. 115–1134, 2001.
- [7] D. Niarchos, "Magnetic MEMS: Key issues and some applications," *Sens. Actuators A*, vol. 109, pp. 166–173, 2003.
- [8] E. Klokholm and J. A. Aboaf, "The measurement of magnetostriction in ferromagnetic thin films," *IEEE Trans. Magn.*, vol. 12, no. 6, pp. 819–821, Nov. 1976.
- [9] E. Klokholm and J. A. Aboaf, "The saturation magnetostriction of permalloy films," *J. Appl. Phys.*, vol. 52, no. 3, pp. 2474–2476, 1981.
- [10] S. Chikazumi, *Physics of Ferromagnetism*, 2nd ed. Oxford, U.K.: Clarendon, 1997.
- [11] C. Kittel, "Physical theory of ferromagnetic domains," *Rev. Mod. Phys.*, vol. 21, p. 541, 1949.
- [12] E. Du Trémolet de Lacheisserie, "Definition and measurement of the surface magnetoelastic coupling coefficients in thin films and multilayers," *Phys. Rev. B*, vol. 51, no. 22, pp. 15 925–15 932, 1995.
- [13] E. Du Trémolet de Lacheisserie and J. C. Peuzin, "Magnetostriction and internal stresses in thin films: The cantilever method revisited," *J. Magn. Mater.*, vol. 136, p. 189, 1994.
- [14] ———, "Magnetostriction and internal stresses in thin films: The cantilever method revisited," *J. Magn. Mater.*, vol. 152, p. 231, 1996.
- [15] V. H. Guerrero and R. C. Wetherhold, "Magnetostrictive bending of cantilever beams and plates," *J. Appl. Phys.*, vol. 94, no. 10, pp. 6659–6666, 2003.
- [16] V. H. Guerrero and R. C. Wetherhold, "Strain and stress calculation in bulk magnetostictive materials and thin films," *J. Magn. Mater.*, vol. 271, pp. 190–206, 2004.
- [17] P. M. Marcus, "Magnetostrictive bending of a film-substrate system," *Phys. Rev. B*, vol. 53, no. 5, pp. 2481–2486, 1996.
- [18] P. M. Marcus, "Magnetostrictive bending of a cantilevered film-substrate system," *J. Magn. Mater.*, vol. 168, pp. 18–24, 1997.
- [19] J. Betz, K. Mackay, and D. Givord, "Magnetic and magnetostrictive properties of amorphous  $Tb_{(1-x)}Co_x$  thin films," *J. Magn. Mater.*, vol. 207, pp. 180–187, 1999.
- [20] R. Watts *et al.*, "Finite-element modeling of magnetostrictive bending of a coated cantilever," *Appl. Phys. Lett.*, vol. 70, no. 19, pp. 2607–2609, 1997.
- [21] COMSOL, MULITPHYSICS © (FEMLAB) (1997–2005). [Online]. Available: <http://www.comsol.com/>
- [22] P. Deuffhard, "A modified Newton method for the solution of ill-conditioned systems of nonlinear equations with applications to multiple shooting," *Number Math*, vol. 22, pp. 289–315, 1974.
- [23] V. H. Guerrero and R. C. Wetherhold, "Magnetostrictively induced vibration of film-substrate plates," *J. Magn. Mater.*, vol. 284, pp. 260–272, 2004.
- [24] N. H. Duc, K. Mackay, J. Betz, and D. Givord, "Giant magnetostriction in amorphous  $(Tb_{1-x}Dy_x)(Fe_{0.45}Co_{0.55})_y$  films," *J. Appl. Phys.*, vol. 79, no. 2, p. 973, 1996.

Manuscript received October 7, 2005; revised November 2, 2005 (e-mail: j.dean@sheffield.ac.uk).